Theoretical investigation of a pressure-induced phase transition in $EuCo_2P_2$

Per H. Andersson, Lars Nordström, Peter Mohn,* and Olle Eriksson
Condensed Matter Theory Group, Department of Physics, University of Uppsala, Box 530, 751 21 Uppsala, Sweden
(Received 10 September 2001; published 23 April 2002)

In this paper we present the findings of a theoretical investigation of the properties of $EuCo_2P_2$ as functions of applied pressure with regards to crystal, electronic, and magnetic structure using full-potential *ab initio* methods. At a moderate applied pressure we observe a phase transformation from a divalent phase to a trivalent high-pressure phase with an associated change of the lattice parameters, which is explained by changes of the electronic structure. With the change of the valence state of Eu a change of the magnetic structure is observed going from localized *f* state magnetism to *d* state magnetism in Co. The theoretical results are in agreement with recent experiments.

DOI: 10.1103/PhysRevB.65.174109 PACS number(s): 71.15.Ap, 71.18.+y, 71.20.Be, 75.30.Fv

I. INTRODUCTION

Of all structures the $ThCr_2Si_2$-type is one of the richest considering the number of different isostructural compounds. One possible explanation for this richness is that this structure can adapt to a variety of different atomic sizes. In this paper we present results on $EuCo_2P_2$ which belongs to a group of phosphides, RT_2P_2 where R=rare earth and T=transition metal. In $EuCo_2P_2$ a phase transition between a phase with long P-P distance and a phase with short P-P distance[1–3] has been observed. This phase transition has been found to be caused by a change in composition, temperature or applied external pressure.

In this paper we have studied the effect of an applied external pressure on the crystal, electronic, and magnetic structure in $EuCo_2P_2$. This material is reported[1,2,4,5] to undergo a structural and magnetic phase transition at a pressure of 3.0 GPa from a long P-P distance phase, with divalent and magnetic Eu and nonmagnetic Co, to a short P-P distance phase with trivalent, nonmagnetic Eu and magnetic Co with an estimated moment of $0.6\mu_B$ at the Co site. A change of the volume as well as a collapse of the c/a ratio are associated with the phase transition. The collapse decreases the P-P distance but increases the Co-Co distance, which together with a charge transfer from Eu and P to Co are suggested in the literature as the mechanisms behind the establishment of moments at the Co site. The reported[6] spin structure for the low-pressure phase is an incommensurate spin spiral with a propagation vector $\mathbf{q}=[0,0,0.85]2\pi/c$, a moment at the Eu site of $6.9\mu_B$ per Eu atom and a Néel temperature of 66.5 K. The intricate structural and magnetic properties, with a transferred magnetism from the Eu atom to the Co atom with varying applied pressure, call for a theoretical analysis. It is the purpose of this paper to provide such an analysis based on first-principles calculations.

The rest of this paper is organized as follows: in Sec. II we describe the theoretical methods used. In Sec. III we present our results and in Sec. IV we summarize our findings.

II. THEORETICAL METHOD

The energy differences involved in these calculations are on the meV scale and the magnetic state is rather complex, involving $4f$ magnetism. This puts high demands on the methods used. To achieve this energy resolution and resolve the magnetic state we have used two different density-functional[7,8] based full-potential methods. For the calculations of the magnetic state we have used a full-potential linear augmented plane-wave (FP-LAPW) method[9,10] in the local spin-density approximation[11] (LSDA) in an implementation that allows for noncollinear magnetism (NCM), that is, the magnetization density is not constrained to polarize parallel or antiparallel to a global direction,[12–14] as well as a noncollinear augmented spherical wave (ASW) method.[15] The latter method implements a similar method for treating noncommensurate orderings as FP-LAPW, but a simpler basis set making the computations less time consuming. For the calculation of the electronic and structural phase transition a full-potential linear muffin-tin orbital method (FP-LMTO),[16,17] in combination with both the local-density approximation (LDA) and the generalized gradient approximation (GGA), was used. The choice of using an FP-LMTO method for calculating the electronic and structural phase transition was of convenience only. The two methods were tested to give the same results.

In the case of FP-LAPW no shape or directional approximations for the magnetization density have been used, i.e., the charge and magnetization densities, as well as their conjugate potentials, are allowed to vary freely in space both in magnitude and direction. The adoption of the spin spiral symmetry[18,19] enables us to handle planar and canted (conical) helical spin structures, where the parallel spins within a plane are rotating around an axis with an angle $\phi=qd/2$ between each plane, where d is the interlayer distance. As the magnetization density is no longer invariant with respect to translations, a generalized boundary condition is used,

$$\vec{m}(\mathbf{r}+\mathbf{R})=\mathcal{D}(\mathbf{q}\cdot\mathbf{R})\vec{m}(\mathbf{r}). \quad (1)$$

Here $\mathbf{R}$ is a Bravais lattice vector, $\mathbf{q}$ is the wave vector of the spin spiral, $\mathbf{q}=[qqq]$ for a trigonal spin spiral and $\mathbf{q}=[00q]$ for a tetragonal spin spiral, and $\mathcal{D}(\mathbf{q}\cdot\mathbf{R})$ is the matrix which performs a rotation by the angle $\mathbf{q}\cdot\mathbf{R}$ around the propagation axis. The generalized Bloch spinors can then be written in the form[18,19]

$$\psi(\mathbf{k},\mathbf{r}) = \begin{pmatrix} \exp(i\{\mathbf{k}-\mathbf{q}/2\}\cdot\mathbf{r})\,\alpha(\mathbf{k},\mathbf{r}) \\ \exp(i\{\mathbf{k}+\mathbf{q}/2\}\cdot\mathbf{r})\,\beta(\mathbf{k},\mathbf{r}) \end{pmatrix}, \quad (2)$$

where $\mathbf{k}$ is a wave vector in the Brillouin zone and α and β are periodic functions for the two spin components. The secular matrix constructed from these states and the magnetic part of the exchange correlation potential $\vec{b}_{\mathrm{xc}}$, which fulfill the same boundary conditions as the magnetization density $\vec{m}$, is no longer block diagonal, i.e., the two spin components are allowed to hybridize. Within the LSDA,[11] the effective magnetic field $\vec{b}_{\mathrm{xc}}$ is always locally parallel to the local magnetization direction. This scheme is made self-consistent by constructing new charge and magnetization densities from the occupied Bloch spinors, for which the necessary Brillouin-zone (BZ) integrations are performed. One large advantage of the spin spiral scheme is that the secular equation has the dimension corresponding to the chemical unit cell irrespective of the size of the magnetic cell, i.e., it allows for noncommensurate ordering.

To sample the Brillouin zone a Fermi-Dirac temperature smearing was used with 100 k points in the irreducible Brillouin zone. The plane-wave cutoff was set to $R_P^{MT}K_{max}=7.0$ for a first sampling of the possible spin solutions and $R_P^{MT}K_{max}=9.0$ close to the most interesting configurations. All states up to $5s$ in Eu, $3p$ in Co, and $2p$ in P have been treated as core states. For the expansion of the valence states $l_{max}=8$ was used.

In the calculations where FP-LMTO was used we adopted a so-called ''double basis'' of muffin-tin orbitals[20,21] where two different tail functions (Hankel or Neumann functions) with different kinetic energies are attached to two different linear combinations of the radial solution to a Schrödinger-like equation for a spherical averaged crystal potential inside each muffin-tin sphere. The radial function is labeled ϕ_ν, and its first energy derivative $\dot{\phi}_\nu$, and they are evaluated at an energy E_ν. The Hamiltonian matrix was thus doubled in size compared to calculations with a single basis. The inclusion of a double basis was necessitated by the fact that a very good energy resolution is required, and to achieve this a well-converged wave function is needed. We have used the same core configuration and l_{max} as for FP-LAPW and 59 k points in the irreducible Brillouin zone.

We have used the experimental values[1] with respect to c/a ratios and atomic positions for all calculations and the experimental volumes for the calculation of the magnetic properties.

III. RESULTS

A. Phase stability, crystal, and electronic structure

As reported[1] $EuCo_2P_2$ undergoes a pressure-induced phase transition at 3.0 GPa accompanied by a change in the valence state of Eu from a magnetic divalent $4f^7$ ($^8S_{7/2}$) state to a nonmagnetic trivalent $4f^6$ ($^7F_0$) state. This type of behavior is well known in rare earths. This phase transition can in principle be calculated, but there exists a subtle problem when comparing total energies from bulk calculations of two different valence states of a rare-earth metal. To evaluate the total energy accurately one needs to calculate the energy of forming the lowest multiplet of a given f configuration. In Ref. 22 it was demonstrated how this can be done and the energy difference between the f^6 and f^7 configurations were calculated using LS coupling, a method that was used here also. In Ref. 22 it was also established that the accuracy of this approach is of the order of 10 mRy.

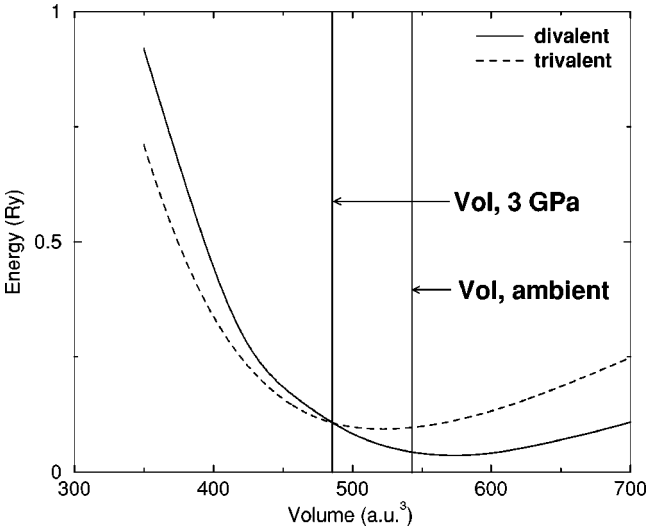

FIG. 1. Total energy as a function of volume for divalent and trivalent spin-polarized $EuCo_2P_2$. The experimental values for the c/a ratio have been used for both phases. The vertical lines indicate the experimental volumes at ambient pressure and just after the phase transition. The choice of zero point in the energy scale is arbitrary.

As can be seen from Fig. 1 the total-energy calculations favor a divalent state at ambient conditions, and as a function of compression there is a phase transition to the trivalent phase (all experimental parameters are from Ref. 1). The calculated pressure for when the trivalent phase is stabilized is 15 GPa, which is to be compared to the experimental value of 3 GPa. However, if a small shift of -10 mRy, which is comparable with the accuracy of the method used for the multiplet correction, is applied to the trivalent curve, the theoretical pressure agrees with the measured one. In the figure we also compare the equilibrium volume as given by the theoretical calculations and experiment as well as the volume for when the phase transition sets in. It may be noted that the agreement between experiment and theory is rather good concerning both these volumes.

In earlier calculations, using a less accurate method[4] it was found that the P $3s$ and $3p$ bands change from the low-pressure phase to the high-pressure phase increasing the bonding strength of the P $3p$ orbitals. They also observed a high density of states (DOS) at the Fermi level. This is in good agreement with the calculations presented in this paper. From the paramagnetic total density of states, Fig. 2, it can be seen that the density of states is high at the Fermi level both for the divalent and the trivalent case. This would indicate a possible moment at the Co site for both cases, but only in the trivalent case a moment at the Co site is observed. This will be discussed in the following section. As a reference,

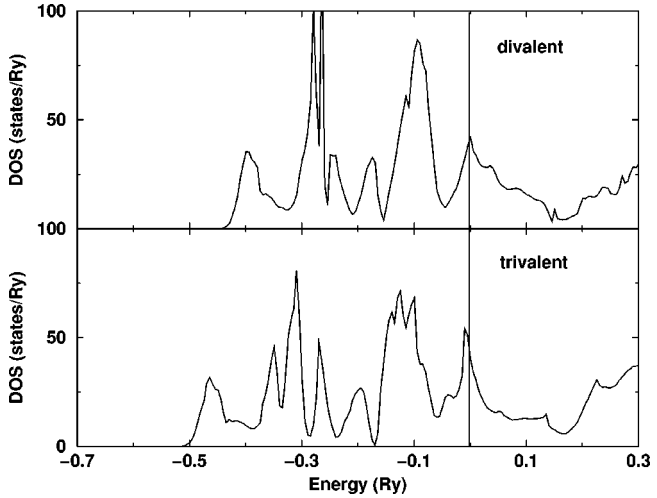

FIG. 2. The total density of states for paramagnetic $EuCo_2P_2$ at ambient pressure (divalent), and at high pressure (trivalent). The Fermi level is at zero energy.

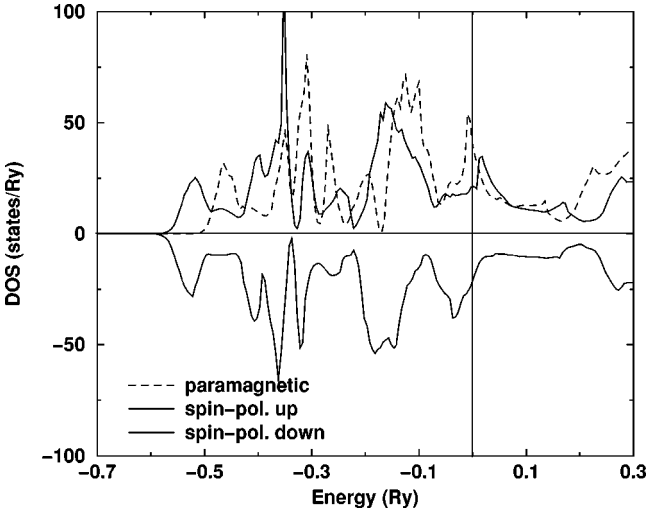

FIG. 3. The total density of states for paramagnetic and spin-polarized $EuCo_2P_2$ at high pressure. The Fermi level is at zero energy.

Fig. 3 shows the density of states for paramagnetic and spin-polarized $EuCo_2P_2$ in the trivalent high-pressure phase.

The volume of the trivalent phase is lower than that of the divalent phase due primarily to the fact that there is one extra bonding electron in the valence band. The reason why the trivalent phase is not stable at ambient conditions is the atomic polarization energy of the *f* shell, which favors the divalent phase. The phase transition from trivalent to divalent can be understood as a balance between the bonding energy, which becomes more favorable at compressed volumes because the bandwidth is increased, and the polarization energy of the *f* shell.

Reehuis *et al.*[3] have reported a relation between the P-P distance and the radius of the rare-earth ion in RT_2P_2 systems, which is in good agreement with the observed results. In the trivalent state the ionic radius of Eu is smaller than in the divalent state, the decrease being of the order of 15%, which leads to a modification of the c/a ratio. In addition, this will lead to an increase in the P—P bonding, which can be seen in the projected density of states for P, Fig. 4, where a slight lowering of the energy of the P $3p$ band can be observed in the high-pressure phase compared to the low-pressure phase. In addition, the bandwidth of the *p* band is broader in the trivalent phase demonstrating the larger overlap between the P *p* states. As can be seen from Fig. 4, the Co and P bands are strongly hybridized below 0.25 Ry, the telltale sign of a covalent bond. The difference between the Eu—Co/P bonds and the Co—P bond is explained by the significant difference in the bond lengths, where the Eu—Co/P bonds are more than 50% longer than the Co—P bond in both phases.

The increased P—P bonding along the *c* axis can also be seen in the charge density (Figs. 5 and 6). These figures represent the charge density in a (110) plane where the Eu ions can be found in the middle and in the corners and the P ions surround the central Eu ion. An increase of charge between the P ions can be observed indicating a stronger bond. This is particularly clear if one considers the two P atoms that lie along the horizontal axis in the figures. A deformation of the Eu-P bond can also be observed, which could change the hybridization between orbitals with different angular dependence favoring certain crystallographic arrangements.[23] This possibility has not been investigated further in this case.

B. Magnetic structure

From the magnetic point of view $EuCo_2P_2$ is of high interest in that the system in the low-pressure phase exhibits localized $4f$ moments at the Eu sites with a complex magnetic ordering,[6] a spin spiral with $\mathbf{q}=[0,0,0.85]2\pi/c$. In the high pressure phase this is replaced by $3d$ magnetism with an estimated moment of $0.6\mu_B$ per Co atom, a suggested ferromagnetic ordering in the Co planes and a complex antiferromagnetic ordering between the planes with a stacking order along the *c* axis of $++--$.[5]

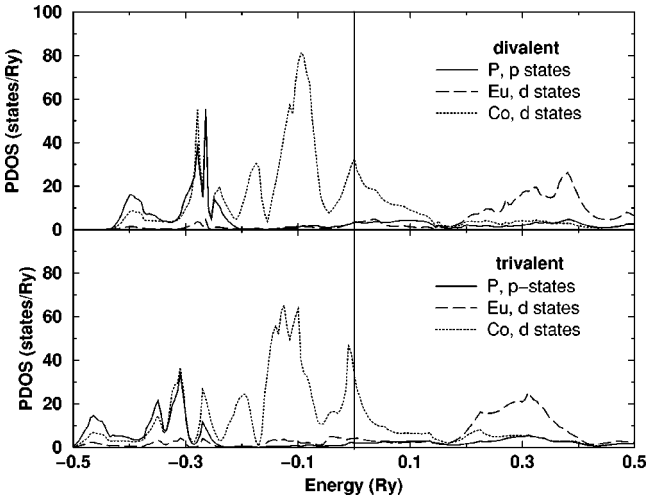

FIG. 4. The projected density of states for P, Eu and C in paramagnetic $EuCo_2P_2$ at ambient pressure (divalent), and at high pressure (trivalent). The Fermi level is at zero energy.

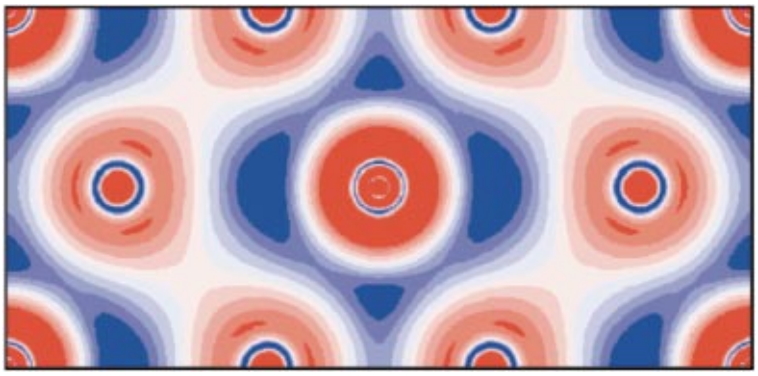

FIG. 5. (Color) The charge density of paramagnetic $EuCo_2P_2$ at ambient pressure (divalent phase). The Eu atoms are located in the corners and in the center and the P atoms surround the central atom. The same absolute scale has been used in Figs. 5 and 6.

As was discussed above the density of states at the Fermi level is high both for the paramagnetic low pressure phase and the paramagnetic high-pressure phase, whereas a moment at the Co site is observed only for the high-pressure phase. This could be explained by a quenching of the $3d$ moments in the divalent phase by the large $4f$ moments, which are arranged almost perfectly antisymmetrically around the Co sites in the ground-state magnetic structure suggested from the experiments. Our calculations for divalent Eu with a ferromagnetically ordered local moment of $7\mu_B$ give a moment at the Co site of $0.2\mu_B$ per Co atom compared to a zero moment at the Co sites for antiferromagnetically ordered local moments at the Eu sites. Calculations using the ASW method resulted in a spin spiral ground state for the divalent phase, with a wave vector of $\mathbf{q}=[0,0,0.89]2\pi/a$ in excellent agreement with experiments.[6] Small changes in the volume only marginally influence the magnetic properties, both as regards the magnetic moments and the q value of the spin spiral.

Since, in the low-pressure phase, the Co d band, with a high DOS at the Fermi level, has a strong tendency to become magnetically ordered, we conclude that this ordering is quenched due to the interaction with the neighboring Eu atoms. Since the Eu atoms are antiferromagnetically ordered, with the Co atoms symmetrically situated in between, any nearest-neighbor collinear magnetic interaction between Eu and Co will lead to frustration. Obviously, the energy of the magnetic frustration of the Co atoms is sufficiently high so that it becomes favorable for Co to maintain its nonmagnetic configuration.

A direct comparison between the spin ordering in the high-pressure phase obtained from experiments and calculations is complicated by the richness of the possible orderings in combination with the lack of a unified experimental picture. Of the possible spin configurations we have investigated ferromagnetic and antiferromagnetic ordering as well as some of the simpler spin spirals. The first configuration is a flat spin spiral, where the spins within a Co plane are ferromagnetically ordered and rotated between planes. Further, we have investigated a configuration where the spins are ordered antiferromagnetically within the Co plane and antiferromagnetically between Co planes. The last configuration investigated is a spin structure where the spins are aligned ferromagnetically within the Co plane and ferromagnetically between two planes but rotated between the pairs. Within the resolution of the method used the ground state for the high pressure, trivalent phase was calculated to be a ferromagnetic configuration. The magnetic moment of the trivalent phase was $0.54\mu_B$ on the Co atom, which is in good agreement with the estimated value of $0.6\mu_B$. For reduced volumes the calculated moments are somewhat smaller.

IV. DISCUSSION

The main results from this paper are in good agreement with experiments regarding the crystal structure, phase trans-

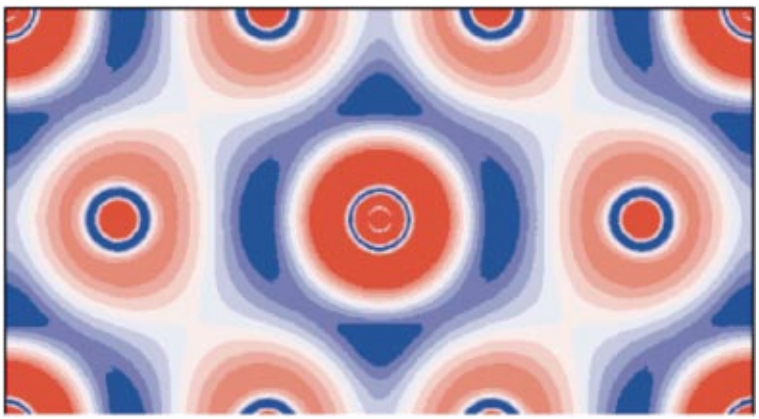

FIG. 6. (Color) The charge density of paramagnetic $EuCo_2P_2$ at high pressure (trivalent phase).

formations, electronic structure, and magnetic states. When a moderate pressure is applied to $EuCo_2P_2$, an up till then localized *f* electron will transfer to delocalized states in the valence band, as in other similar rare earth materials, and the volume will be reduced. In the case of $EuCo_2P_2$ the reduction of the volume comes in the form of a collapse of the *c* axis and even a small increase of the *a* axis. This can be explained by the change in the volume of the Eu ion, and a rearrangement of the electronic structure leading to a stronger P—P bond, which decreases the P—P distance and therefore causes a shorter *c* axis.

In the low-pressure phase the magnetic moment is caused by the localized *f* electrons with the ground state of $^8S_{7/2}$, a magnetic configuration with a calculated helical spin ordering of $\mathbf{q}=[0,0,0.89]2\pi/a$. The strong moment of Eu in an antiferromagnetic configuration has been calculated to quench the moments of Co. In the high-pressure phase the electronic state of the Eu *f* electrons is $^7F_0$, a nonmagnetic state. In this phase a moment is observed at the Co sites in good agreement with experiments, and it is consistent with what one expects for Co compounds where the *d* band intersects the Fermi level. The ordering of the moments in the trivalent phase has been calculated, but the lack of a conclusive experimental result for the magnetic structure prevents a direct comparison. A vast computational effort is needed to examine the possible configuration space and is outside the scope of the present paper.

Tha actual phase transition may involve domain structures where parts of the sample contain divalent Eu atoms and other parts trivalent atoms. This scenario is plausible not only for the current system but may be more general, e.g., in pressure-induced structural phase transitions of nonmagnetic materials. Here we have not made a mesoscopic analysys of the phase transition in $EuCo_2P_2$, but calculated its electronic origin.

ACKNOWLEDGMENTS

The support from The Swedish Science Council (VR) and The Swedish Foundation for Strategic Research (SSF) is appreciated. We are grateful to Dr. J. M. Wills for providing the FP-LMTO code. We are also grateful to Dr. Anna Delin for valuable discussions.

*Permanent address: Center for Computational Science, Vienna University of Technology, A-1060 Vienna, Austria.

[1] C. Huhnt, W. Schlabitz, A. Wurth, A. Mewis, and M. Reehuis, Phys. Rev. B **56**, 13 796 (1997).
[2] C. Huhnt, W. Schlabitz, A. Wurth, A. Mewis, and M. Reehuis, Physica B **252**, 44 (1998).
[3] M. Reehuis, W. Jeitschko, G. Kotzyba, B. Zimmer, and X. Hu, J. Alloys Compd. **266**, 54 (1998).
[4] B. Ni, M. Abd-Elmeguid, H. Micklitz, J. Sanchez, P. Vulliet, and D. Johrendt, Phys. Rev. B **63**, 100102 (2001).
[5] M. Chefki, M. Abd-Elmeguid, H. Micklitz, C. Huhnt, W. Schlabitz, M. Reehuis, and W. Jeitschko, Phys. Rev. Lett. **80**, 802 (1998).
[6] M. Reehuis, W. Jeitschko, M. Möller, and P. Brown, J. Phys. Chem. Solids **53**, 687 (1992).
[7] P. Hohenberg and W. Kohn, Phys. Rev. **136**, B864 (1964).
[8] W. Kohn and L. Sham, Phys. Rev. **140**, A1133 (1965).
[9] O. Andersen, Phys. Rev. B **12**, 3060 (1975).
[10] D. Singh, *Planewaves, Pseudopotentials, and the LAPW Method* (Kluwer Academic, Dordrecht, 1994).
[11] U. von Barth and L. Hedin, J. Phys. C **5**, 1629 (1972).
[12] J. Kübler, K.-H. Höck, J. Sticht, and A. R. Williams, J. Phys. F: Met. Phys. **18**, 469 (1988).
[13] L. M. Sandratskii and P. G. Guletskii, J. Phys. F: Met. Phys. **16**, 43 (1986).
[14] L. Nordström and D. J. Singh, Phys. Rev. Lett. **76**, 4420 (1996).
[15] M. Uhl, L. M. Sandratskii, and J. Kübler, J. Magn. Magn. Mater. **103**, 314 (1992).
[16] J. Wills and B. Cooper, Phys. Rev. B **36**, 3809 (1987).
[17] J. M. Wills, O. Eriksson, M. Alouani, and D. L. Price, *Electronic Structure and Physical Properties of Solids* (Springer, Berlin, 2000).
[18] L. Sandratskii, Phys. Status Solidi B **135**, 167 (1986).
[19] C. Herring, *Magnetism* (Academic Press, New York, 1966), Vol. 4.
[20] O. K. Andersen, Phys. Rev. B **12**, 3060 (1975).
[21] H. H. Skriver, *The LMTO Method* (Springer, Berlin, 1984).
[22] A. Delin, L. Fast, B. Johansson, J. Wills, and O. Eriksson, Phys. Rev. Lett. **79**, 4637 (1997).
[23] P. H. Andersson, L. Fast, L. Nordström, B. Johansson, and O. Eriksson, Phys. Rev. B **58**, 5230 (1998).